HHS Public Access

Author manuscript

Clin Imaging. Author manuscript; available in PMC 2017 September 01.

Published in final edited form as:

Clin Imaging. 2016 ; 40(5): 1009–1013. doi:10.1016/j.clinimag.2016.05.009.

Microstructural Maturation of White Matter Tracts in Encephalopathic Neonates

Akash P. Kansagra, M.D., M.S.[a], **Marc C. Mabray, M.D.**[b], **Donna M. Ferriero, M.D., M.S.**[c], **A. James Barkovich, M.D.**[b,c], **Duan Xu, Ph.D.**[b], and **Christopher P. Hess, M.D., Ph.D.**[b]

[a]Mallinckrodt Institute of Radiology, Washington University School of Medicine (510 S. Kingshighway Blvd., Campus Box 8131, Saint Louis, MO 63110)

[b]Department of Radiology and Biomedical Imaging, University of California, San Francisco (505 Parnassus Avenue, M-391, San Francisco, CA 94143)

[c]Departments of Pediatrics and Neurology, University of California, San Francisco (400 Parnassus Avenue, San Francisco, CA 94143)

Abstract

Purpose—To apply neurite orientation dispersion and density imaging (NODDI) to measure white matter microstructural features during early development.

Methods—NODDI parameters were measured in twelve newborns and thirteen 6 month infants, all with perinatal clinical encephalopathy.

Results—Between 0 and 6 months, there were significant differences in fractional anisotropy (FA) for all tracts; in neurite density for internal capsules, optic radiations, and splenium; and in orientation dispersion for anterior limb of internal capsule and optic radiations. There were no appreciable differences in NODDI parameters related to outcome.

Conclusion—NODDI may allow more detailed characterization of microstructural maturation than FA.

Keywords

brain; maturation; microstructure; diffusion tensor imaging; magnetic resonance imaging; pediatrics

1. INTRODUCTION

MRI has proved an invaluable tool for assessing the developing neonatal brain. However, MRI may be apparently normal even in neonates with clinically obvious signs of encephalopathy [1], presumably reflecting the presence of microscopic injury, particularly in

Corresponding author: Akash P. Kansagra, M.D., M.S., 510 S. Kingshighway Blvd, Campus Box 8131, Saint Louis, MO 63110, +1-314-362-5949 (phone), +1-314-362-4886 (fax), apkansagra@gmail.com.

white matter tracts that are most susceptible to disruption by early neurological insult [2–7]. Better imaging tools are thus needed to identify neonatal brain injury and abnormal maturation at a microscopic scale.

Much of the work to develop such tools has centered on diffusion tensor imaging (DTI). Unfortunately, conventional processing of DTI data yields metrics such as fractional anisotropy (FA) that are sensitive to microstructure but cannot readily discriminate between the different components of microstructure [8–10]. A newer DTI method termed neurite orientation dispersion and density imaging (NODDI) can better discriminate microstructural features such as the density of axons and dendrites (collectively, “neurites”), fiber tract organization, and free water content [11–13].

In this study, we use NODDI to characterize white matter microstructural parameters in encephalopathic neonates born at term. Specifically, we measure neurite density (ND), orientation dispersion (OD), and free water fraction (FW) in major white matter tracts at birth and at six months of life, discuss how differences in NODDI parameters vary by tract, and compare NODDI parameters between infants with different neurological outcomes.

2. METHODS

2.1. Subjects

The study was initiated following approval by the institutional review board. Inclusion criteria for enrollment were: (a) birth at or after 36 weeks gestation; (b) moderate to severe encephalopathy identified by an attending neonatologist or pediatric neurologist; and (c) Apgar score less than 5 at 10 minutes of life, prolonged resuscitation at birth, pH of less than 7.0 in any blood sample taken within 60 minutes of birth, or base deficit greater than 12 mmol/L in any cord or arterial blood sample taken within 60 minutes of birth. Exclusion criteria were: (a) evidence of *in utero* or perinatal infection, (b) major anomalies of the brain or other major organ systems, or (c) evidence of congenital metabolic disease. For ethical and feasibility reasons, normal controls (i.e., infants born without encephalopathy) were not enrolled in the study.

Written informed consent was obtained for all subjects to be enrolled in a program of clinical neurological follow up and undergo brain MRI including research sequences. A total of twenty-five infants underwent brain imaging with a NODDI-compatible protocol (Table 1); twelve of these subjects were imaged in the first week of life and thirteen were imaged at six months of life. Clinical neuromotor development was assessed using the last documented neurological examination, with each infant being assigned a validated neuromotor score [14]—0 for normal development, 1 for abnormal tone or reflexes, 2 for abnormal tone and reflexes, 3 for functional deficit of power, 4 for cranial nerve involvement with motor abnormality, and 5 for spastic quadriparesis. All infants in this study had neuromotor scores of 0 or 1 an average of 318 days after birth. Longitudinal imaging evaluation with serial MRIs was not considered appropriate in these infants with no or mild neurological impairment.

2.2. Data acquisition and processing

MR imaging was performed on 3.0 Tesla GE magnets (Discovery MR750 or Signa HDxt, General Electric Medical Systems, Milwaukee, WI, USA) using a commercially available 8-channel head coil. Infants were sedated during image acquisition with intravenous propofol under the supervision of a trained anesthesiologist. Diffusion MRI data was acquired in each subject using a two-shell high angular resolution diffusion imaging (HARDI) protocol with ASSET acceleration factor 2, and spatial resolution of 2 × 2 × 2 mm. Inner shell data were acquired in 30 directions with b=700 s/mm^2, TR=5000 ms, and TE=62.1–68.3 ms in the 0 month group, and b=700 s/mm^2, TR=8000–12500 ms, and TE=68.8–80.5 ms in the 6 month group. Outer shell data were acquired in 55 directions with b=2000 s/mm^2, TR=6000 ms, and TE=77.1–85.9 ms in the 0 month group, and b=2000 s/mm^2 or 3000 s/mm^2, TR=11000–14500 ms, and TE=87.3–109.5 ms in the 6 month group. Each HARDI shell was supplemented by an additional b=0 s/mm^2 volume acquired using the same TR and TE. This supplemental volume was used to normalize the HARDI data in order to compensate for variable TR and TE. Total HARDI acquisition time was approximately 3 minutes for the inner shell and 5 minutes for the outer shell.

Diffusion data were corrected for motion and eddy current artifacts using the FMRIB Software Library [15]. Inner shell HARDI data were used to calculate FA maps, after which the complete set of two-shell HARDI data were processed using the NODDI Matlab toolbox (University College London) [11]. NODDI analysis yielded whole-brain maps of OD, ND, and FW.

2.3. ROI analysis

ROIs were manually drawn on axial and sagittal FA maps by a neuroradiologist within the anterior and posterior limbs of the internal capsule (ALIC and PLIC); optic radiations; and genu, body, and splenium of the corpus callosum (Figure 1). This neuroradiologist was blinded to the NODDI maps during ROI selection. ROIs could not be drawn in one neonate due to excessive motion artifact, reducing to twenty-four the number of subjects included in the analysis. In these remaining subjects, ROIs were automatically translated to co-registered NODDI parameter maps, and mean values of FA, OD, ND, and FW were calculated within each ROI for each subject.

Statistical analysis of ROI data was performed in Matlab 2013a (The Mathworks Inc., Natick, MA). Groupwise analysis of differences between was performed using Student's two-tailed *t* test. Statistical significance in the face of multiple comparisons was determined using the Benjamini-Hochberg method and a false discovery rate of 5% over 24 independent comparisons (4 parameters in each of 6 ROIs) [16]. Statistical comparison of the corpus callosum to ALIC, PLIC, and optic radiations at birth was also performed using Student's two-tailed *t* test.

3. RESULTS

Microstructural maps for two typical subjects are shown in Figure 2. Qualitatively, maps of OD depict the known locations of highly organized white matter tracts and show

correspondingly low values in these regions even at birth, as would be expected given the reciprocal relationship between OD and FA. ND demonstrates comparatively less heterogeneity across each image, though there is slightly higher ND in the subcortical white matter shortly after birth that disappears by six months of age. Maps of FW show large values within the ventricles and subarachnoid spaces, with very low values within the brain substance at term.

Microstructural indices—FA, OD, ND, and FW—were measured within each selected white matter tract (Table 2). At 0 months, the corpus callosum collectively demonstrated significantly higher FA than the ALIC or optic radiations ($p<0.05$). Moreover, the corpus callosum demonstrated significantly lower OD and higher FW than the PLIC, ALIC, or optic radiations at birth ($p<0.05$).

Measured FA was significantly higher at 6 months than at 0 months within all measured white matter tracts. In contrast, ND was significantly higher only within the PLIC, ALIC, optic radiations, and splenium. Furthermore, OD was significantly higher only within the ALIC and optic radiations. Measured FW was significantly lower at 6 months than at 0 months in the optic radiations, genu, and splenium.

To identify potential relationships between imaging and neurological outcomes, FA and NODDI indices at 6 months were further assessed using subgroup analysis based on neuromotor outcomes (Table 3). There were no statistically significant differences in FA or NODDI parameters related to neuromotor scores.

4. DISCUSSION

Previous studies have attempted to characterize the microstructural changes of maturation by measuring the evolution of FA or related anisotropy metrics that are known to be dependent on tissue microstructure [2, 17–20]. However, the relationship between FA and underlying microstructure is complex and influenced by a number of factors, including fiber orientation, axonal diameter, myelination, free water content, and cellular infiltrates in response to infection or injury [21–24]. As such, the insights that can be attained through FA alone are limited.

Several groups have developed alternate DTI-based metrics that have different sensitivities to various microstructural features compared to FA [19, 24, 25]. In combination with FA, these metrics confer an improved ability to disentangle the competing effects of multiple underlying microstructural changes on the overall diffusion signal. In so doing, they have clarified the timing of maturational changes, including identification of a “premyelination” phase that precedes myelin-related changes on T1- or T2-weighted imaging [7, 26]. By comparison, NODDI uses a three-compartment tissue model to map the observed diffusion signal directly into parameters of OD, ND, and FW [11]. These parameters are more intuitively appealing as markers of tissue architecture, and emerging evidence suggests that they accurately reflect histological features of the underlying brain [12, 13, 27].

To our knowledge, no other studies have yet described changes in NODDI parameters in the immediate postnatal phase. Despite significantly higher FA in all measured white matter

tracts at the end of the first six months of life, we found corresponding significant ND differences only within the PLIC, ALIC, optic radiations, and splenium, and significant OD differences only within the ALIC and optic radiations. Observed differences in FW in the corpus callosum are presumed to reflect smaller partial volume effects in the larger, 6 month old brain.

We speculate that these tract-to-tract differences in NODDI parameter changes reflect more basic processes of physiological and structural development. MRI and histological studies have consistently shown an ordered sequence of white matter myelination, involving the PLIC and optic radiations at or near term, the splenium and ALIC within 1–4 months post-term, and the body and genu of the corpus callosum beginning at approximately 6 months post-term [28–32]. The magnitude of ND increase we measured in each tract—large in the PLIC, optic radiations, and ALIC; intermediate in the splenium; and small in the genu and body—matches this known myelination sequence. In this context, the small ND change in the genu and body presumably reflects the comparatively early stage of myelin maturation in these structures at 6 months, which marks the end of our observational period. These observations also corroborate earlier results that suggest that FA increases in the splenium occur earlier than in the remainder of the corpus callosum, presumably due to relatively later maturation of myelin in the genu and body [33, 34].

One of the primary motivations for studying NODDI in encephalopathic infants is the hypothesized ability to more accurately detect and characterize subtle microstructural abnormalities that may occur in this population. Applying NODDI in these patients shortly after birth may thus improve our understanding of the biophysical basis of perinatal injury and ability to predict eventual neurological outcome. Recently, Lally and colleagues showed that term infants with moderate or severe encephalopathy at birth exhibited significantly lower FA and radial diffusivity in white matter tracts compared to term infants with no or mild encephalopathy [35, 36]. However, using a single-shell NODDI model, the authors demonstrated that these differences in FA and radial diffusivity were the result of lower white matter ND in encephalopathic infants, as there was no appreciable difference in OD between these groups [35, 36]. Thus, while DTI-based metrics such as FA may indicate the presence of a microstructural abnormality, NODDI-derived parameters can add important new insights by resolving these abnormalities into tissue component features (e.g., ND and FW) and geometrical organization (e.g., OD) [12, 37, 38]. The importance of decreased ND in encephalopathic infants has been underscored by subsequent work demonstrating that decreased ND—but not OD—is predictive of poorer neurological outcomes [39]. Aside from elucidating the nature of injury, these results offer promise for improved neurodevelopmental prognostication shortly after birth.

Our outcomes-based subgroup analysis did not demonstrate any discernible differences in NODDI parameters between encephalopathic infants with normal neurological development (neuromotor score of 0) and encephalopathic infants with mild neurological impairment (neuromotor score of 1), suggesting that microstructural differences between these two groups is small. Encephalopathic infants with more severe neurological impairment (neuromotor scores of 2–5), which were not represented in our study, may exhibit more obvious differences in NODDI parameters—presumably decreased ND without significantly

altered OD, as in recent work using a single-shell NODDI model [35, 36, 39]—and thus may be a useful target population for future studies.

Curiously, our data provide some evidence that the presence of encephalopathy may itself affect NODDI parameters, regardless of ultimate neurological outcome. In particular, the OD and ND values that we measure in infants with encephalopathy appear considerably lower than in normal infants [37], while corroborating the results of Lally and colleagues suggesting that OD in encephalopathic neonates is likely to be less than 0.1 in areas such as the corpus callosum with FA above 0.4 [36]. Though minor differences in ROI selection and DTI acquisition can influence the accuracy of NODDI and FA estimates in different patient groups, the fact that our measurements of FA in encephalopathic patients—measurements which are derived from the same DTI source data and ROIs used for NODDI analysis—are in good agreement with published FA values from non-encephalopathic infants [18, 19, 34, 37] implies that the actual influence of these technical factors is minimal, and therefore, that observed differences in NODDI parameters are reliable.

A limitation of this study is that the ages of the subjects are not uniformly distributed between 0 and 6 months, but rather are clustered around these two time points. This approach is appropriate to gain a general understanding of microstructural development but obscures the multiphasic temporal evolution that has been noted in other studies [25, 34, 40, 41]. A second limitation was that imaging was performed with acquisition parameters chosen to maximize signal-to-noise ratio and minimize acquisition time. For example, we changed the outer shell b value partway through the study in order to increase diffusion signal. This change was considered unlikely to affect NODDI estimates, as Zhang et al. have shown that different two-shell acquisition protocols with outer shell b value ranging from 2000–3000 s/mm^2 yield very similar NODDI results [11]. In addition, we preferred to use the minimum TE for each diffusion acquisition and allowed minor variation of this parameter between patients. The effect of these variations on the resulting diffusion signal were offset by normalizing each diffusion volume by a b=0 s/mm^2 volume acquired with the same TE. Variations in TR were related to the number of slices needed for complete coverage of the brain. A third limitation is that encephalopathic infants with moderate or severe neurological impairment were not studied, which may obscure microstructural abnormalities that are normal or only very minimally abnormal in the less impaired population of infants included in our analysis.

These limitations notwithstanding, we have demonstrated differences in NODDI microstructural parameters during the first six months of life. Regional variation in observed NODDI parameters differences may correspond to known differences in the timing of myelination between these structures. Thus, NODDI or other related methods that can accurately characterize tissue microstructure may prove useful for characterizing subtle brain injury, and in so doing may improve our ability to predict neurological outcomes in infants that have experienced early neurological insult.

5. CONCLUSION

We have characterized differences in NODDI microstructural indices in major white matter tracts of encephalopathic term neonates during the first six months of life. Despite higher FA in all measured white matter tracts at 6 months of life, differences in NODDI indices between 0 and 6 months demonstrate tract-to-tract variability that may reflect regional variation in myelination over this time period. NODDI parameters were similar in encephalopathic infants with normal neurological development and those with mild neurological impairment. Methods such as NODDI may hold promise for detecting and characterizing abnormal microstructural maturation and may lead to improved understanding of the nature of early neurological insult.

Acknowledgments

National Institutes of Health T32 EB001631, R01 EB9756, HD 72074, NS 046432, NS 35902

References

1. Miller SP, Ramaswamy V, Michelson D, Barkovich AJ, Holshouser B, Wycliffe N, et al. Patterns of brain injury in term neonatal encephalopathy. J Pediatr. 2005; 146(4):453–60. [PubMed: 15812446]
2. Miller SP, Vigneron DB, Henry RG, Bohland MA, Ceppi-Cozzio C, Hoffman C, et al. Serial quantitative diffusion tensor MRI of the premature brain: development in newborns with and without injury. J Magn Reson Imaging. 2002; 16(6):621–32. [PubMed: 12451575]
3. Volpe JJ. Cerebral white matter injury of the premature infant-more common than you think. Pediatrics. 2003; 112(1 Pt 1):176–80. [PubMed: 12837883]
4. Salmaso N, Jablonska B, Scafidi J, Vaccarino FM, Gallo V. Neurobiology of premature brain injury. Nat Neurosci. 2014; 17(3):341–6. [PubMed: 24569830]
5. Back SA, Miller SP. Brain injury in premature neonates: A primary cerebral dysmaturation disorder? Ann Neurol. 2014; 75(4):469–86. [PubMed: 24615937]
6. Volpe JJ. Brain injury in premature infants: a complex amalgam of destructive and developmental disturbances. Lancet Neurol. 2009; 8(1):110–24. [PubMed: 19081519]
7. Huppi PS, Dubois J. Diffusion tensor imaging of brain development. Semin Fetal Neonatal Med. 2006; 11(6):489–97. [PubMed: 16962837]
8. Pierpaoli C, Jezzard P, Basser PJ, Barnett A, Di Chiro G. Diffusion tensor MR imaging of the human brain. Radiology. 1996; 201(3):637–48. [PubMed: 8939209]
9. Alexander AL, Lee JE, Lazar M, Field AS. Diffusion tensor imaging of the brain. Neurotherapeutics. 2007; 4(3):316–29. [PubMed: 17599699]
10. Winston GP. The physical and biological basis of quantitative parameters derived from diffusion MRI. Quant Imaging Med Surg. 2012; 2(4):254–65. [PubMed: 23289085]
11. Zhang H, Schneider T, Wheeler-Kingshott CA, Alexander DC. NODDI: practical in vivo neurite orientation dispersion and density imaging of the human brain. Neuroimage. 2012; 61(4):1000–16. [PubMed: 22484410]
12. Counsell SJ, Ball G, Edwards AD. New imaging approaches to evaluate newborn brain injury and their role in predicting developmental disorders. Curr Opin Neurol. 2014; 27(2):168–75. [PubMed: 24561870]
13. van de Looij Y, Dean JM, Gunn AJ, Huppi PS, Sizonenko SV. Advanced magnetic resonance spectroscopy and imaging techniques applied to brain development and animal models of perinatal injury. Int J Dev Neurosci. 2015; 45:29–38. [PubMed: 25818582]
14. Hajnal BL, Sahebkar-Moghaddam F, Barnwell AJ, Barkovich AJ, Ferriero DM. Early prediction of neurologic outcome after perinatal depression. Pediatr Neurol. 1999; 21(5):788–93. [PubMed: 10593667]

15. Jenkinson M, Beckmann CF, Behrens TE, Woolrich MW, Smith SM. FSL. Neuroimage. 2012; 62(2):782–90. [PubMed: 21979382]
16. Benjamini Y, Hochberg Y. Controlling the false discovery rate: a practical and powerful approach to multiple testing. J R Stat Soc Ser B Stat Methodol. 1995; 57(1):289–300.
17. Mukherjee P, Miller JH, Shimony JS, Conturo TE, Lee BC, Almli CR, et al. Normal brain maturation during childhood: developmental trends characterized with diffusion-tensor MR imaging. Radiology. 2001; 221(2):349–58. [PubMed: 11687675]
18. Hermoye L, Saint-Martin C, Cosnard G, Lee SK, Kim J, Nassogne MC, et al. Pediatric diffusion tensor imaging: normal database and observation of the white matter maturation in early childhood. Neuroimage. 2006; 29(2):493–504. [PubMed: 16194615]
19. Partridge SC, Mukherjee P, Henry RG, Miller SP, Berman JI, Jin H, et al. Diffusion tensor imaging: serial quantitation of white matter tract maturity in premature newborns. Neuroimage. 2004; 22(3): 1302–14. [PubMed: 15219602]
20. Partridge SC, Vigneron DB, Charlton NN, Berman JI, Henry RG, Mukherjee P, et al. Pyramidal tract maturation after brain injury in newborns with heart disease. Ann Neurol. 2006; 59(4):640–51. [PubMed: 16450369]
21. Jones DK, Knosche TR, Turner R. White matter integrity, fiber count, and other fallacies: the do's and don'ts of diffusion MRI. Neuroimage. 2013; 73:239–54. [PubMed: 22846632]
22. Rose SE, Hatzigeorgiou X, Strudwick MW, Durbridge G, Davies PS, Colditz PB. Altered white matter diffusion anisotropy in normal and preterm infants at term-equivalent age. Magn Reson Med. 2008; 60(4):761–7. [PubMed: 18816850]
23. Yoshida S, Oishi K, Faria AV, Mori S. Diffusion tensor imaging of normal brain development. Pediatr Radiol. 2013; 43(1):15–27. [PubMed: 23288475]
24. Mukherjee P, Miller JH, Shimony JS, Philip JV, Nehra D, Snyder AZ, et al. Diffusiontensor MR imaging of gray and white matter development during normal human brain maturation. AJNR Am J Neuroradiol. 2002; 23(9):1445–56. [PubMed: 12372731]
25. Dubois J, Dehaene-Lambertz G, Perrin M, Mangin JF, Cointepas Y, Duchesnay E, et al. Asynchrony of the early maturation of white matter bundles in healthy infants: quantitative landmarks revealed noninvasively by diffusion tensor imaging. Hum Brain Mapp. 2008; 29(1):14–27. [PubMed: 17318834]
26. Prayer D, Barkovich AJ, Kirschner DA, Prayer LM, Roberts TP, Kucharczyk J, et al. Visualization of nonstructural changes in early white matter development on diffusion-weighted MR images: evidence supporting premyelination anisotropy. AJNR Am J Neuroradiol. 2001; 22(8):1572–6. [PubMed: 11559509]
27. Sepehrband F, Clark KA, Ullmann JF, Kurniawan ND, Leanage G, Reutens DC, et al. Brain tissue compartment density estimated using diffusion-weighted MRI yields tissue parameters consistent with histology. Hum Brain Mapp. 2015; 36(9):3687–702. [PubMed: 26096639]
28. Barkovich AJ, Kjos BO, Jackson DE Jr, Norman D. Normal maturation of the neonatal and infant brain: MR imaging at 1.5 T. Radiology. 1988; 166(1 Pt 1):173–80. [PubMed: 3336675]
29. Bird CR, Hedberg M, Drayer BP, Keller PJ, Flom RA, Hodak JA. MR assessment of myelination in infants and children: usefulness of marker sites. AJNR Am J Neuroradiol. 1989; 10(4):731–40. [PubMed: 2505502]
30. Paus T, Collins DL, Evans AC, Leonard G, Pike B, Zijdenbos A. Maturation of white matter in the human brain: a review of magnetic resonance studies. Brain Res Bull. 2001; 54(3):255–66. [PubMed: 11287130]
31. Brody BA, Kinney HC, Kloman AS, Gilles FH. Sequence of central nervous system myelination in human infancy. I. An autopsy study of myelination. J Neuropathol Exp Neurol. 1987; 46(3):283–301. [PubMed: 3559630]
32. Kinney HC, Brody BA, Kloman AS, Gilles FH. Sequence of central nervous system myelination in human infancy. II. Patterns of myelination in autopsied infants. J Neuropathol Exp Neurol. 1988; 47(3):217–34. [PubMed: 3367155]
33. Gilmore JH, Lin W, Corouge I, Vetsa YS, Smith JK, Kang C, et al. Early postnatal development of corpus callosum and corticospinal white matter assessed with quantitative tractography. AJNR Am J Neuroradiol. 2007; 28(9):1789–95. [PubMed: 17923457]

34. Gao W, Lin W, Chen Y, Gerig G, Smith JK, Jewells V, et al. Temporal and spatial development of axonal maturation and myelination of white matter in the developing brain. AJNR Am J Neuroradiol. 2009; 30(2):290–6. [PubMed: 19001533]

35. Lally PJ, Zhang H, Pauliah SS, Price DL, Bainbridge A, Cady EB, et al. Microstructural changes in neonatal encephalopathy revealed with the neurite orientation dispersion and density imaging (NODDI) model. Arch Dis Child Fetal Neonatal Ed. 2014; 99:A14.

36. Lally, PJ.; Zhang, H.; Pauliah, SS.; Price, DL.; Bainbridge, A.; Cady, EB., et al. Neurite orientation dispersion and density imaging (NODDI) adds biophysical insight of white matter microstructural injury in neonatal encephalopathy. International Society of Magnetic Resonance in Medicine; Milan, Italy: 2014. p. 2673

37. Kunz N, Zhang H, Vasung L, O'Brien KR, Assaf Y, Lazeyras F, et al. Assessing white matter microstructure of the newborn with multi-shell diffusion MRI and biophysical compartment models. Neuroimage. 2014; 96:288–99. [PubMed: 24680870]

38. Jelescu IO, Veraart J, Adisetiyo V, Milla SS, Novikov DS, Fieremans E. One diffusion acquisition and different white matter models: how does microstructure change in human early development based on WMTI and NODDI? Neuroimage. 2015; 107:242–56. [PubMed: 25498427]

39. Lally PJ, Zhang H, Pauliah SS, Price DL, Bainbridge A, Cady EB, et al. Neurite density index correlates with childhood neurological outcome after neonatal encephalopathy. Neonatal Society. 2014

40. Zanin E, Ranjeva JP, Confort-Gouny S, Guye M, Denis D, Cozzone PJ, et al. White matter maturation of normal human fetal brain. An in vivo diffusion tensor tractography study. Brain Behav. 2011; 1(2):95–108. [PubMed: 22399089]

41. Sadeghi N, Prastawa M, Fletcher PT, Wolff J, Gilmore JH, Gerig G. Regional characterization of longitudinal DT-MRI to study white matter maturation of the early developing brain. Neuroimage. 2013; 68:236–47. [PubMed: 23235270]

Highlights

- In all white matter tracts, fractional anisotropy changed between 0 and 6 months.
- Neurite density and orientation dispersion only changed in some tracts.
- No parameter differences were found between mildly impaired and unimpaired infants.
- These patterns of change may reflect the known timing of myelination in each tract.

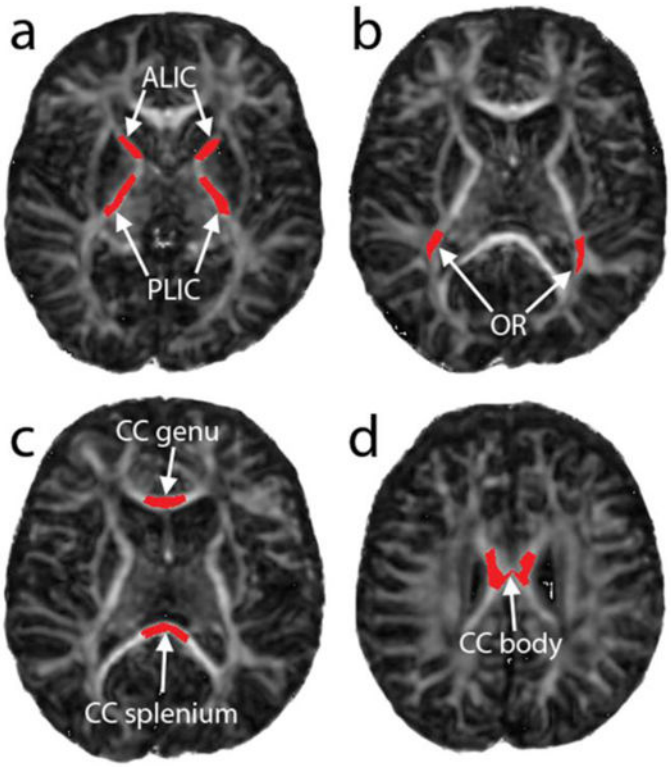

Figure 1.
Fractional anisotropy maps with superimposed ROIs corresponding to (a) anterior and posterior limbs of the internal capsule, (b) optic radiations, (c) genu and splenium of corpus callosum, and (d) body of corpus callosum.

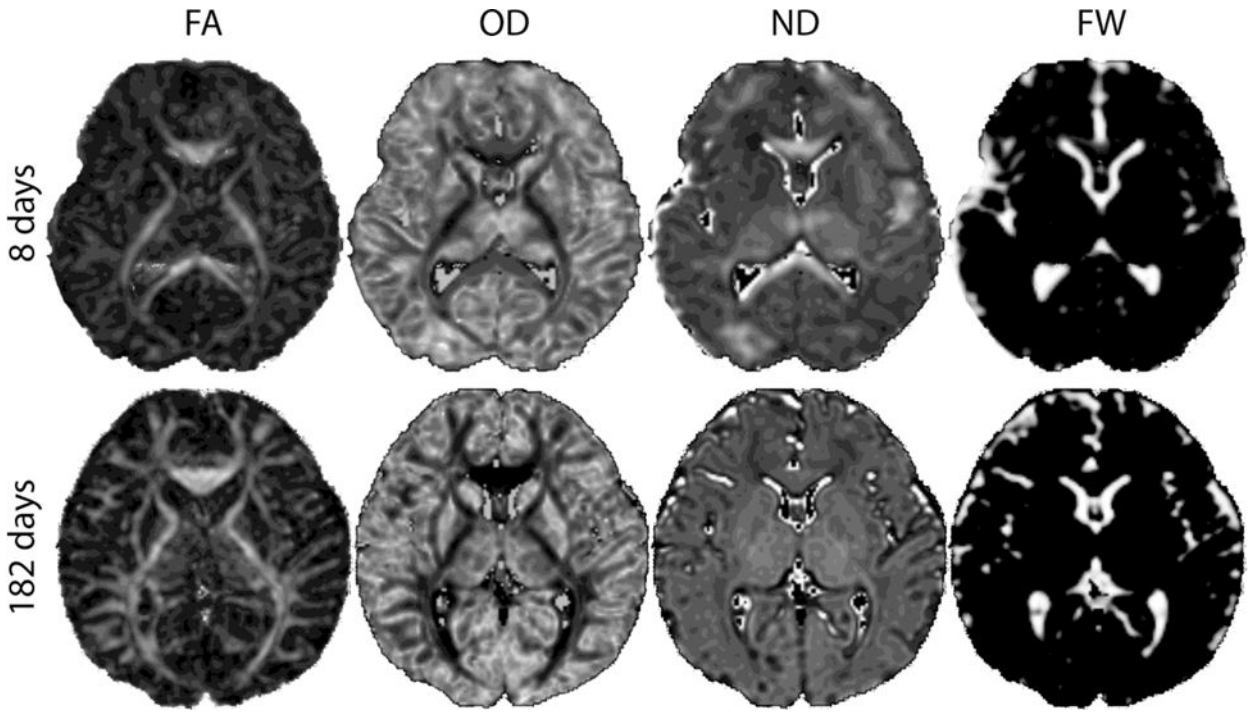

Figure 2.

NODDI parameter maps in two representative subjects, one shortly after birth (top row) and one at 6 months (bottom row). Images are scaled to similar size. FA = fractional anisotropy, OD = orientation dispersion, ND = neurite density, FW = free water fraction.

Table 1

Subject characteristics. Standard deviations are indicated in parenthesis.

	0 months	6 months
Corrected birth age (days)	−6.4 (10.5)	−4.4 (7.4)
Gender	55% male	46% male
5 minute Apgar	4.6 (1.6)	4.5 (2.2)
Seizures	18%	8%
Neuromotor score	0.36 (0.50)	0.23 (0.44)

Table 2

NODDI microstructural parameters at 0 months and 6 months. Standard deviations are indicated in parenthesis. Asterisks denote statistical significance.

	Tract[†]	0 months	6 months	*p*
FA	PLIC	0.443 (0.049)	0.602 (0.049)	<0.001*
	ALIC	0.306 (0.042)	0.445 (0.084)	<0.001*
	OR	0.347 (0.042)	0.447 (0.047)	<0.001*
	CC genu	0.511 (0.060)	0.672 (0.048)	<0.001*
	CC body	0.492 (0.060)	0.578 (0.035)	<0.001*
	CC splenium	0.597 (0.053)	0.770 (0.044)	<0.001*
ND	PLIC	0.287 (0.033)	0.435 (0.037)	<0.001*
	ALIC	0.208 (0.038)	0.354 (0.028)	<0.001*
	OR	0.179 (0.063)	0.329 (0.039)	<0.001*
	CC genu	0.270 (0.107)	0.302 (0.054)	0.392
	CC body	0.221 (0.060)	0.255 (0.049)	0.149
	CC splenium	0.315 (0.104)	0.402 (0.042)	0.021*
OD	PLIC	0.097 (0.027)	0.109 (0.021)	0.093
	ALIC	0.131 (0.052)	0.168 (0.043)	0.014*
	OR	0.108 (0.051)	0.160 (0.025)	<0.001*
	CC genu	0.043 (0.048)	0.054 (0.024)	0.492
	CC body	0.048 (0.048)	0.048 (0.024)	0.982
	CC splenium	0.049 (0.060)	0.042 (0.019)	0.717
FW	PLIC	0.000 (0.000)	0.000 (0.000)	1.000
	ALIC	0.000 (0.000)	0.000 (0.000)	0.163
	OR	0.001 (0.001)	0.000 (0.000)	0.011*
	CC genu	0.127 (0.097)	0.015 (0.023)	0.003*
	CC body	0.051 (0.048)	0.039 (0.052)	0.572
	CC splenium	0.080 (0.071)	0.011 (0.012)	0.009*

[†]OR = optic radiation, CC = corpus callosum.

Table 3

NODDI microstructural parameters at 0 months in infants with neuromotor scores (NMS) of 0 or 1. Standard deviations are indicated in parenthesis.

	Tract[†]	Normal[‡]	Encephalopathic		
			NMS = 0	NMS = 1	*p*
FA	PLIC	0.50 (0.02)	0.45 (0.04)	0.42 (0.05)	0.150
	ALIC	0.37 (0.04)	0.30 (0.04)	0.31 (0.04)	0.533
	OR	0.32 (0.03)	0.36 (0.04)	0.33 (0.04)	0.083
	CC genu	0.54 (0.05)	0.52 (0.05)	0.49 (0.07)	0.466
	CC body	0.46 (0.05)	0.50 (0.06)	0.47 (0.06)	0.441
	CC splenium	0.61 (0.03)	0.60 (0.05)	0.59 (0.06)	0.714
ND	PLIC	0.39 (0.03)	0.28 (0.03)	0.29 (0.05)	0.710
	ALIC	0.30 (0.03)	0.21 (0.03)	0.20 (0.05)	0.793
	OR	0.23 (0.03)	0.17 (0.03)	0.19 (0.10)	0.765
	CC genu	0.38 (0.03)	0.28 (0.09)	0.26 (0.15)	0.859
	CC body	0.45 (0.06)	0.20 (0.04)	0.26 (0.08)	0.226
	CC splenium	0.45 (0.03)	0.29 (0.04)	0.35 (0.17)	0.566
OD	PLIC	0.17 (0.01)	0.09 (0.02)	0.11 (0.03)	0.040
	ALIC	0.22 (0.02)	0.13 (0.05)	0.13 (0.06)	0.809
	OR	0.26 (0.03)	0.10 (0.02)	0.12 (0.08)	0.459
	CC genu	0.15 (0.02)	0.03 (0.01)	0.07 (0.08)	0.438
	CC body	0.20 (0.04)	0.04 (0.04)	0.06 (0.06)	0.600
	CC splenium	0.13 (0.02)	0.03 (0.02)	0.08 (0.10)	0.385
FW	PLIC	0.01 (0.01)	0.00 (0.00)	0.00 (0.00)	1.000
	ALIC	0.01 (0.01)	0.00 (0.00)	0.00 (0.00)	0.307
	OR	0.02 (0.02)	0.00 (0.00)	0.02 (0.03)	0.205
	CC genu	0.18 (0.05)	0.17 (0.09)	0.05 (0.03)	0.015
	CC body	0.26 (0.11)	0.06 (0.05)	0.03 (0.02)	0.161
	CC splenium	0.17 (0.04)	0.11 (0.07)	0.03 (0.02)	0.035

[†]OR = optic radiation, CC = corpus callosum.

[‡]Normal reference data from Ref. [37].